Journal of Luminescence 143 (2013) 108–112

Contents lists available at SciVerse ScienceDirect

Journal of Luminescence

journal homepage: www.elsevier.com/locate/jlumin

Enhanced efficiency in single-host white organic light-emitting diode by triplet exciton conversion

Qingyang Wu [a,*,1], Shiming Zhang [a,b,1], Shouzhen Yue [a], Zhensong Zhang [a], Guohua Xie [c], Yi Zhao [a,*,2], Shiyong Liu [a]

[a] State Key laboratory on Integrated Optoelectronics, College of Electronic Science and Engineering, Jilin University, Changchun 130012, People's Republic of China
[b] Département of Chemical Engineering, École Polytechnique de Montréal, Montréal, Québec, Canada H3C3J7
[c] Institut für Angewandte Photophysik, Technische Universtität Dresden, Dresden 01062, Germany

ARTICLE INFO

Article history:
Received 14 February 2013
Accepted 18 April 2013
Available online 29 April 2013

Keywords:
WOLED
Single host
EQE
FIrpic
PO-01
Co-dope

ABSTRACT

The authors observe that the external quantum efficiency (EQE) of the Iridium (III) bis(4-phenylthieno [3,2-c]pyridinato-N,$C^{2'}$)acetylacetonate (PO-01) based yellow organic light-emitting diode (OLED) is significantly increased by uniformly co-doping Iridium (III)bis[(4,6-difluorophenyl)-pyridinato-N,C^{2-}] (FIrpic) and PO-01 into the same wide band-gap host of N,N′-dicarbazolyl-3, 5-benzene (mCP). Detailed investigation indicates that the efficiency enhancement is ascribed to effective triplet exciton gathering by FIrpic, followed by energy transfer to PO-01. Compared to the control device, which has maximum EQE of 10.5%, an improved maximum EQE of 13.2% is obtained in the optimization white device based on FIrpic and PO-01 emission according to this principle. This work makes it easier for a single host white OLED to simultaneously harvest high efficiency in both blue and yellow units. Comprehensive experimental results show that this phenomenon can also be found and utilized in other popular hosts to realize more efficient white devices.

1. Introduction

Phosphorescent white organic light-emitting diodes (WOLEDs) have drawn particular attention due to their potential applications in solid-state lighting, flat panel display and the unique merits of high external quantum efficiency (EQE) and environmental friendliness, which have a positive effect on the reduction of greenhouse gases [1–4]. Although the state-of-the-art phosphorescent WOLEDs have achieved attractive improvements in efficiencies and lifetimes [5], paving the way for commercial production, further improvement is required to simplify the device structure in order to reduce the production costs and make the technology competitive against other alternative technologies such as inorganic LEDs [6–10]. Among approaches to simplify the device structure, adopting the same host for different emitters to act as a single white emission layer (SWEML) has great potential because it can significantly lower the driving voltage and yield a much higher brightness at low applied voltage due to the reduction of total number of organic layers in the devices, rendering it more easier to be compatible with the conventional driving techniques. [8,9,11] However, as is known, it is relatively arduous to acquire such a phosphorescent host material, which is suitable for both the blue and yellow/red emitters to simultaneously realize high efficiency. In particular, the blue phosphorescent emitter has a more rigorous demand on the hosts because the latter must simultaneously offer suitable frontier molecular orbital energy levels, wide band-gap (E_g) and high lowest triplet-excited states (T_1) to ensure efficient carrier transport as well as exothermic energy transfer to the emitter molecule [12]. Therefore, the blue-favorite host with a wide E_g is often prior adopted in the SWEML devices [8,13,14], which may cause a considerable efficiency loss in the red/yellow unit inevitably.

N,N′-dicarbazolyl-3, 5-benzene (mCP) has been extensively used as a host material for the classical blue phosphorescent material of Iridium (III)bis[(4, 6-difluorophenyl)-pyridinato-N,C^{2-}] (FIrpic), [8,13] whereas our studies indicate that it is not a very suitable host for yellow Iridium (III)bis(4-phenylthieno[3,2–c]pyridinato-N, $C^{2'}$)acetylacetonate (PO-01) phosphor. In this work, we report the achievement of high efficiency simplified SWEML WOLEDs based on triplet exciton conversion (TEC) process [9], whereby the efficiency of PO-01-doped mCP yellow device is dramatically enhanced. Detailed study suggests that the enhanced efficiency is ascribed to effective triplet exciton gathering by FIrpic from mCP, followed by energy transfer to PO-01. Significantly, our research results indicate that this phenomenon can also be found

* Corresponding authors. Tel.: +86 431 85168242.
E-mail address: wqy1527@163.com (Q. Wu), yizhao@jlu.edu.cn (Y. Zhao).
[1] These authors contributed equally to this work.
[2] Tel.: +86 431 85168242 8301.

0022-2313/$ - see front matter © 2013 Elsevier B.V. All rights reserved.
http://dx.doi.org/10.1016/j.jlumin.2013.04.037

and utilized in other popular hosts, e.g., 4,4′,4″-tris(N-carbazolyl) triphenylamine (TCTA) and 4,4′-N,N′-dicarbazole-biphenyl (CBP). According to this principle, a peak forwarding-viewing EQE, power efficiency (PE) and current efficiency (CE) of 13.9%, 38.3 lm/W and 38.4 cd/A, respectively, with a low voltage of 2.5 V for onset and 4 V at 1000 cd/m^2 is obtained in the optimization SWEML WOLED without any out-coupling enhancements.

2. Experimental, results and discussions

All the devices were fabricated with the conventional process. [15] The current density–voltage–luminance (*J–V–L*) characteristics, electroluminance (EL) spectra and Commission Internationale de L'Eclairage (CIE) coordinates were measured with a PR650 Spectrascan spectrometer and a Keithley 2400 programmable voltage–current source. Correlated color temperature (CCT) values were calculated with software SETFOS 3.0 from FLUXIM AG. The absorption spectrum of PO-01 was measured by means of a UV–vis spectrometer (UV 3600, Shimadzu). The devices were measured only in the forward direction without the use of an integrating sphere and additional out-coupling enhancements.

Simplified devices with the following configurations were fabricated: Y1, Indium Tin Oxide (ITO)/MoO_3 (10 nm)/TCTA (60 nm)/*mCP*: *6% PO-01* (15 nm)/Bphen (50 nm)/LiF (1 nm)/Al (100 nm); Y2, ITO/MoO_3 (10 nm)/TCTA (60 nm)/*mCP*: *15% FIrpic: 6% PO-01* (15 nm)/Bphen (50 nm)/LiF (1 nm)/Al (100 nm); Y3, ITO/MoO_3 (10 nm)/TCTA (60 nm)/*mCP: 0.6% PO-01* (15 nm)/Bphen (50 nm)/LiF (1 nm)/Al (100 nm); and Y4, ITO/MoO_3 (10 nm)/TCTA (60 nm)/*mCP*: *15% FIrpic: 0.6% PO-01* (15 nm)/Bphen (50 nm)/LiF (1 nm)/Al (100 nm). For all devices, MoO_3 is used as the hole injection layer [16], 4,7-diphenyl-1,10-phenanthroline (Bphen) is the electron transport layer (ETL) and hole blocking layer, LiF is the electron injection layer, and Al is the cathode. Fig. 1 shows the structure and energy level diagram of the devices studied; the energy levels are extracted from literatures [13,17,18].

Fig. 2 shows the *J–V–L* curves for various devices shown in Fig. 1. It can be seen that the devices exhibit discriminating *J–V* characteristics. The current density of the FIrpic and PO-01 co-doped devices (Y2, Y4) is significantly higher than that of the solely PO-01 doped control devices (Y1, Y3), whereas a reduction in current density is observed in the device with lower PO-01 doping concentration (Y3). This is because FIrpic in mCP offers good transport channels for both holes and electrons [19], while doping PO-01 into mCP can obviously promote electron transport, which has been proved by the electron-only device as shown in Fig. 3. In addition, as the hole-only device shown in Fig. 3, PO-01 also acts as obvious trapping sites for holes, which indicates that there may exist two different excitation mechanisms for PO-01 in mCP: self-recombination by carrier trapping and energy transfer from mCP to PO-01. [20]

Fig. 4(a) shows the normalized EL spectra and Fig. 4(b) shows the CE, PE and EQE versus luminance plots for devices Y1–Y4. It is clear that spectra of devices Y1–Y3 are exactly the same as that of PO-01 standard device without any FIrpic emission, whereas only a weak FIrpic emission can be observed in device Y4. Significantly, compared to the control device Y1, which has maximum EQE of 10.2%, the co-doped device Y2 shows a more noticeable value of 12.2%, while device Y4 exhibits a rather high EQE of 11.0% compared to the extreme low value of 2.7% in the solely doped control device Y3. To ascertain the optimal FIrpic dosage, we fabricated devices with different FIrpic doping concentrations: ITO/MoO_3 (10 nm)/TCTA (60 nm)/*mCP: x% FIrpic: 6% PO-01* (15 nm)/Bphen (50 nm)/LiF (1 nm)/Al (100 nm), where *x* is set to 15, 30, 40, and 50, respectively. The inset of Fig. 4(b) shows the maximum EQE of the devices as a function of FIrpic doping concentration, a high EQE of 14.1% (CE of 46.0 cd/A), which is even superior to that of the conventional CBP based PO-01 emission device (CE of 43.6 cd/A) [21], is observed in the optimization device with 40% FIrpic doping concentration. Self-quenching of FIrpic will be aggravated at higher doping concentration, which should account for the observed EQE degradation [22].

To reveal the hidden reasons for the EQE enhancement in above devices, we examined the detailed energy transfer processes taking place in the EML by comparing the absorption spectra of FIrpic and PO-01, and the photoluminescence (PL) and phosphorescence spectra of mCP and FIrpic (Fig. 5) [23,24]. From Fig. 5, we can clearly see that the metal-to-ligand charge transfer bands from singlet (^{1}MLCT) and triplet (^{3}MLCT) in PO-01 are clearly resolved at 450 and 508 nm, respectively, whereas the ^{1}MLCT and ^{3}MLCT transitions are, respectively, observed at 380 and 420 nm for FIrpic. There is a large spectra overlap between the PL/phosphorescence spectra of mCP and the ^{3}MLCT and ^{1}MLCT of FIrpic, but only a very small overlap can be observed between that of mCP and PO-01. However, significantly, we note that the ^{1}MLCT and ^{3}MLCT of PO-01 overlaps rather well with the emission spectrum of FIrpic. Based on the above facts, we conclude that the EQE enhancements in the co-doped devices are mainly because the Dexter energy transfer (DET) from T_1 of mCP to FIrpic, followed by energy transfer from T_1 of FIrpic to either the T_1 of PO-01 or to the singlet-excited states of PO-01, which then transits to the T_1 of PO-01 via rapid intersystem crossing, along with a completion of TEC

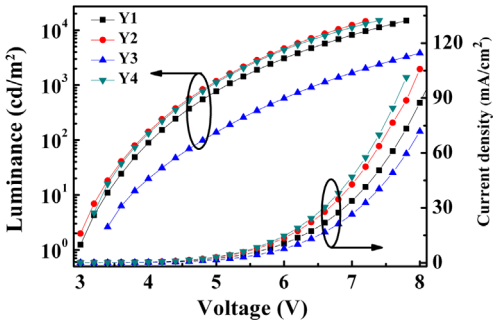

Fig. 2. *V–J–L* curves for devices Y1–Y4.

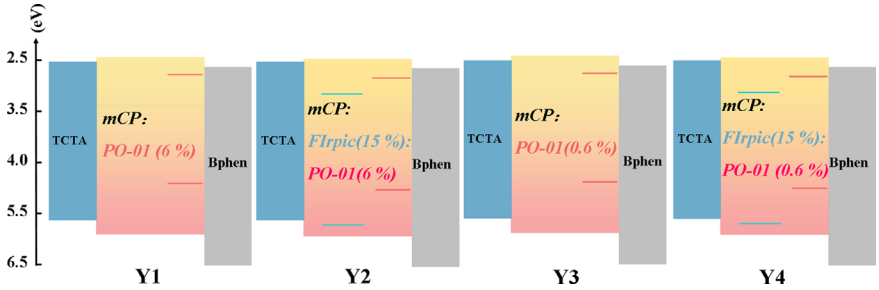

Fig. 1. Device structure and energy bands for devices Y1–Y4.

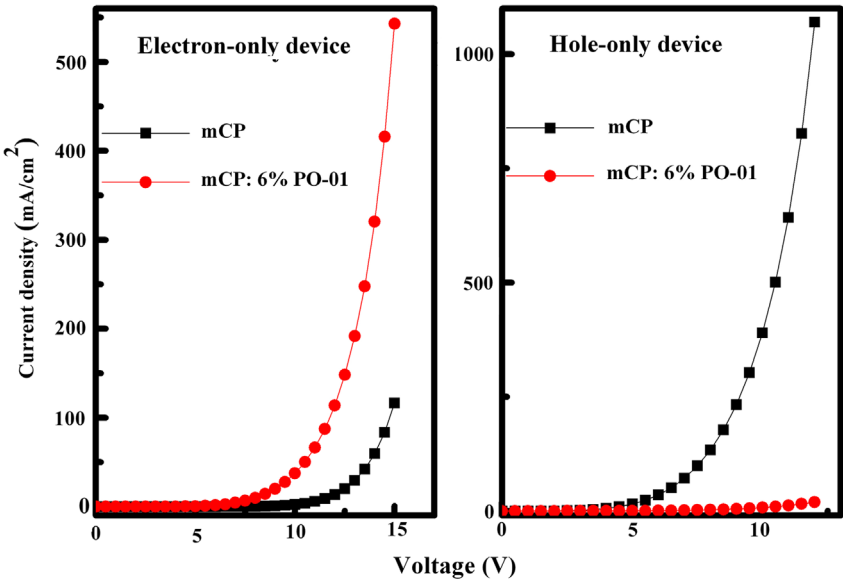

Fig. 3. *J–V* curves of electron-only device (left) with structures of ITO/LiF (1 nm)/Bphen (50 nm)/X (15 nm)/Bphen (50 nm)/LiF (1 nm)/Al (100 nm) and hole-only device (right) with structures of ITO/MoO_x (10 nm)/TCTA (60 nm)/X (15 nm)/TCTA (60 nm)/MoO_x (10 nm)/Al (100 nm). Here X refer to mCP and mCP: 6% PO-01.

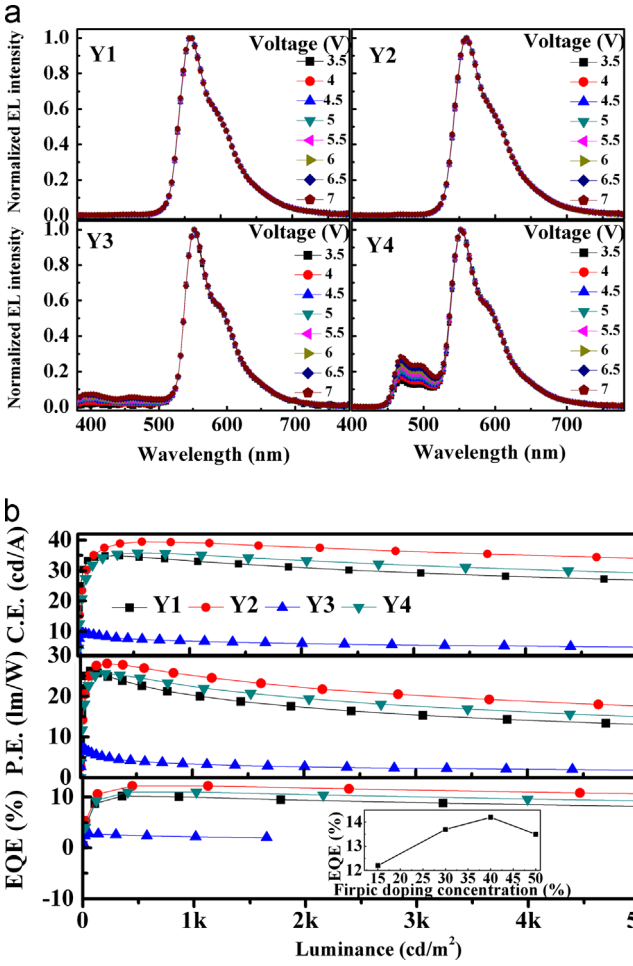

Fig. 4. (a) Normalized EL spectra of devices Y1, Y2,Y3 and Y4 at different applied voltages; (b) CE, PE and EQE versus luminance for devices Y1–Y4, inset shows peak EQE comparison with various FIrpic doping concentrations.

process from FIrpic to PO-01. Moreover, compared to control device Y3, we deduce that the Förster resonance energy transfer (FRET) from FIrpic to PO-01 should be the pivotal reason for the

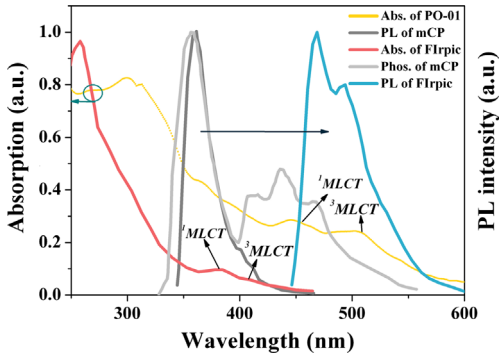

Fig. 5. The normalized PL/phosphorescence (Phos.) spectra of mCP and FIrpic and absorption (Abs.) spectra of PO-01 and FIrpic.

explosive EQE enhancement in device Y4 because the self-recombination of PO-01 and DET from both mCP and FIrpic to PO-01 should be insufficient owing to the low doping concentration (0.6%) of PO-01, which not only strongly restricts the hole trapping behavior of PO-01 but also causes the lumophores to lie beyond the DET radius of an excited mCP molecule [23]. In this case, FRET should be the primary energy transfer process between mCP and PO-01 in device Y3, however, the extremely low EQE (peak value of 2.6%) implies that this process is also inefficient, which further indicates that the FRET from mCP to PO-01 should be inefficient in device Y4. To identify the presumed long-distance energy transfer contribution from FIrpic to PO-01, we first investigate the average exciton distribution profile in the device and disclose that the triplet excitons are mainly located at the mCP/Bphen interface (see upper inset of Fig. 6). In succession, we placed the PO-01 yellow EML at the mCP/Bphen interface and fabricated devices with the following structure: ITO/MoO_3 (10 nm)/TCTA (60 nm)/*mCP* (15–*x* nm), *mCP: 10% FIrpic* (*x* nm), *mCP: 6% PO-01* (5 nm)/Bphen (50 nm)/LiF (1 nm)/Al (100 nm), $x=0$, 1, 3, and 5 for devices S1, S2, S3, and S4, respectively. The thin FIrpic EML acted as a detecting layer (DL). Fig. 6 shows the absolute irradiance spectra of devices S1, S2, S3 and S4. We can see that the FIrpic DL can significantly enhance PO-01 emission intensity with little effect on the carrier transport (see lower inset of Fig. 6). Therefore, this enhancement should be caused only by energy transfer taking place in the EML. However, compared to device S3 (3 nm DL), the

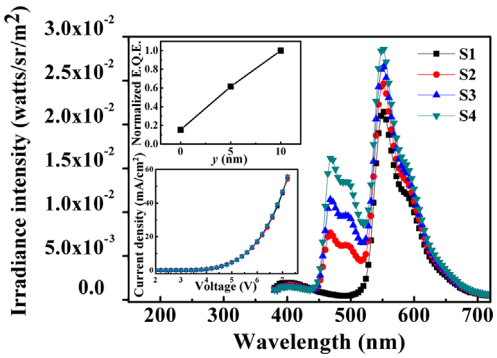

Fig. 6. Absolute irradiance spectra of devices S1–S4 at a current density of 15 mA cm^2. The upper inset shows the average triplet exciton distribution profile (normalized EQE) within mCP host measured at the same current density of 1 mA cm^2 for devices with the structure of ITO/MoOx (10 nm)/TCTA (60 nm)/mCP (*y* nm), mCP: 15% FIrpic (5 nm), mCP (10–*y* nm)/Bphen (50 nm)/LiF (1 nm)/Al (100 nm); The lower inset shows the *J*–*V* characteristics of devices S1–S4.

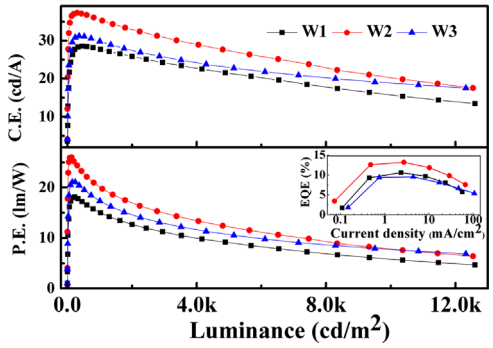

Fig. 7. CE and PE versus luminance for devices W1–W3. Inset shows EQE versus current density curves for devices W1–W3.

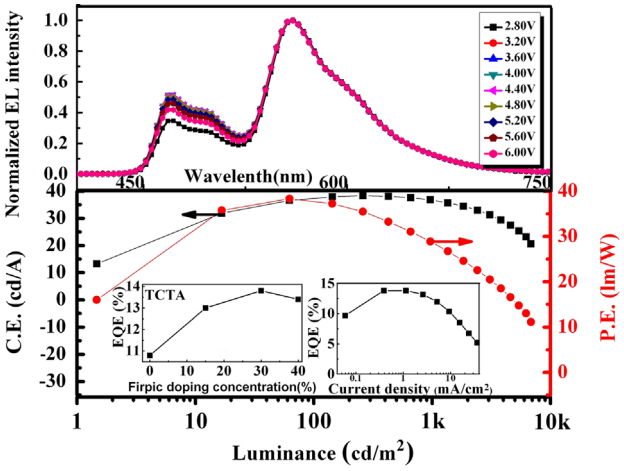

Fig. 8. CE and PE versus luminance of the SWEL white device based on TCTA host: ITO/MoO_x (10 nm)/NPB (50 nm)/TCTA: 30% FIrpic: 6% PO-01 (15 nm)/TCTA: 10% FIrpic (5 nm)/3TPYMB (5 nm)/Bphen (45 nm)/LiF (1 nm)/Al (100 nm). Inset left shows peak EQE comparison of devices employing TCTA host with various FIrpic doping concentrations; inset right shows EQE versus current density and the upper shows the normalized EL spectra of the white device at different applied voltages.

additional 2 nm DL in device S4 cannot transfer the energy to PO-01 via DET because it has already exceeded the DET radius (2 nm) [25]. Thus, the FRET from FIrpic to PO-01 (or PL of PO-01 excited by Firpic), which has a longer critical transfer distance [26], should be responsible for the emission enhancement of PO-01. In fact, the FIrpic DL herein functions as an exciton harvester that gathers portions of excitons diffusing from the yellow EML (mCP/Bphen interface), which are then being retransferred back again from FIrpic to PO-01, thereby significantly enhancing PO-01 emission.

The excellent performance of the co-doped yellow emission device inspired us to further investigate the performance of mCP as the SWEML for simplified WOLEDs. Since mCP and FIrpic both have higher T_1 values than Bphen and 5 nm electron-transporting tri[3-(3-pyridyl)mesityl]-borane (3TPYMB) [27], which has a much higher T_1 value (2.95 eV), was inserted between the EML and BPhen layers as an exciton-blocking layer to prevent the diffusion of T_1 exciton from EML to ETL. This led to the construction of three white devices, the configurations of which were, W1, ITO/MoO_3 (10 nm)/TCTA (60 nm)/*mCP: 6% PO-01* (6 nm)/*mCP: 10% FIrpic* (14 nm)/3TPYMB (5 nm)/Bphen (45 nm)/LiF (1 nm)/Al (100 nm); W2, ITO/MoO_3 (10 nm)/TCTA (60 nm)/*mCP: 40% FIrpic: 6% PO-01* (6 nm)/*mCP: 10% FIrpic* (14 nm)/3TPYMB (5 nm)/Bphen (45 nm)/LiF (1 nm)/Al (100 nm); W3, ITO/MoO_3 (10 nm)/TCTA (60 nm)/*mCP: 40% FIrpic: 6% PO-01* (6 nm)/*mCP: 10% FIrpic* (14 nm)/Bphen (50 nm)/LiF (1 nm)/Al (100 nm). Fig. 7 shows the CE, PE and EQE for devices W1–W3. Compared to the solely doped control device W1, which has maximum EQE, PE and CE of 10.5%, 18.2 lm/W and 28.5 cd/A, respectively, the co-doped device W2 shows an improved performance with maximum EQE, PE and CE of 13.2%, 26.0 lm/W and 37.3 cd/A. The CIE coordinates of W2 shift from (0.35,0.45) to (0.33,0.43) over the illumination-relevant luminance range of 100–1000 cd/m^2 with warm CCT values around 5000 K.

In order to test whether this principle can be utilized for other wide E_g host and fully exploit the merit of this strategy, devices employing the host of TCTA, which is also proved to be a suitable host for FIrpic [5],were fabricated and further studied: ITO/MoOx (10 nm)/NPB (50 nm)/*TCTA: m% FIrpic: 6% PO-01* (20 nm)/3TPYMB (5 nm)/Bphen (45 nm)/LiF (1 nm)/Al (100 nm). As shown in Fig. 8 inset, compared to the solely PO-01 doped control device, which has a peak EQE of 10.7%, the co-doped device with 30% FIrpic doping concentration shows a peak EQE of 13.8%, which is nearly 1.3-fold higher than that of the control device. A maximum EQE, PE and CE of 13.9%, 38.3 lm/W and 38.4 cd/A, respectively, with a low voltage of 2.5 V for onset and 4 V at 1000 cd/m^2 (CCT of 4300 K) is obtained in the optimization WOLED based on TCTA SWEML. The CIE coordinates show only a slight shift from (0.39,0.45) to (0.38,0.45) as the luminance varied from 100 cd/m^2 to 1000 cd/m^2. Moreover, even in CBP, which is a very promising host for PO-01, the EQE enhancement can still be observed by employing this co-doped strategy. The efficiency of the device will be drastically improved by adopting p–i–n structure to further reduce the turn-on voltage as well as achieve more balanced carrier injection or using a periodic outcoupling structure to increase the light extraction [5,16,28].

3. Conclusions

In conclusion, the study presented herein reports on a strategy to boost the efficiency of SWEML WOLEDs by utilizing TEC from FIrpic to PO-01. Accordingly, high efficiency simplified SWEML WOLEDs are demonstrated. Further, this strategy may also solve the color-shift issue over the entire operational lifetime of the device owing to the great emission dependence of PO-01 on FIrpic. It is anticipated that the simple design concept can be applicable to other efficient hosts (especially for wide E_g) and this work might be a significant reference for further research toward high performance SWEML WOLEDs. We anticipate seeing more efficient SWEML WOLEDs based on this study in the future.

Acknowledgments

This work was supported by the National Basic Research Program of China (973 Program) under Grant No. 2010CB327701 and the National Natural Science Foundation of China (Grant Nos. 60977024 and 61275033).

References

[1] M.A. Baldo, D.F. O'Brien, Y. You, A. Shoustikov, S. Sibley, M.E. Thompson S.R. Forrest, Nature 395 (1998) 151.
[2] Y. Ma, H. Zhang, J. Shen, C. Che, Synth. Met. 94 (1998) 245.
[3] B.W. D'Andrade, M.E. Thompson, S.R. Forrest, Adv. Mater. 14 (2002) 147.
[4] B.W. D'Andrade, S.R. Forrest, Adv. Mater. 16 (2004) 1585.
[5] S. Reineke, F. Lindner, G. Schwartz, N. Seidler, K. Walzer, B. Lussem, K. Leo, Nature 459 (2009) 234.
[6] K.T. Kamtekar, A.P. Monkman, M.R. Bryce, Adv. Mater. 22 (2010) 572.
[7] M.C. Gather, A. Köhnen, K. Meerholz, Adv. Mater. 23 (2011) 233.
[8] Q. Wang, J. Ding, D. Ma, Y. Cheng, L. Wang, F. Wang, Adv. Mater. 21 (2009) 2397.
[9] Y.-L. Chang, S. Yin, Z. Wang, M.G. Helander, J. Qiu, L. Chai, Z. Liu, G.D. Scholes, Z. Lu, Adv. Funct. Mater. 23 (2013) 705.
[10] Z.B. Wang, M.G. Helander, J. Qiu, D.P. Puzzo, M.T. Greiner, Z.W. Liu, Z.H. LuAppl. Phys. Lett. 98 (2011) 073310.
[11] Y. Sun, N.C. Giebink, H. Kanno, B. Ma, M.E. Thompson, S.R. Forrest, Nature 440 (2006) 908.
[12] C. Han, G. Xie, H. Xu, Z. Zhang, L. Xie, Y. Zhao, S. Liu, W. Huang, Adv. Mater. 23 (2011) 2491.
[13] G. Xie, Z. Zhang, Q. Xue, S. Zhang, Y. Luo, L. Zhao, Q. Wu, P. Chen, B. Quan, Y. Zhao, S. Liu, J. Phys. Chem. C 115 (2010) 264.
[14] C. Han, Z. Zhang, H. Xu, S. Yue, J. Li, P. Yan, Z. Deng, Y. Zhao, P. Yan, S. Liu, J. Am. Chem. Soc. 134 (2012) 19179.
[15] S. Zhang, G. Xie, Q. Xue, Z. Zhang, L. Zhao, Y. Luo, S. Yue, Y. Zhao, S. Liu, Thin Solid Films 520 (2012) 2966.
[16] G.H. Xie, Y.L. Meng, F.M. Wu, C. Tao, D.D. Zhang, M.J. Liu, Q. Xue, W. Chen, Y. Zhao, Appl. Phys. Lett. 92 (2008) 093305.
[17] S. Kumar, S.M. Shen, S.H. Chen, C.C. Wang, C.C. Chen, J.H. Jou, High efficiency… diodes, in: Proceedings of the IACSIT Coimbatore Conferences 28 (2012) (2012) pp.117–121.
[18] S.W. Liu, Y. Divayana, A.P. Abiyasa, S.T. Tan, H.V. Demir, X.W. Sun, Appl. Phys. Lett. 101 (2012) 093301.
[19] J. Zhao, J. Yu, X. Hu, M. Hou, Y. Jiang, Thin Solid Films 520 (2012) 4003.
[20] M.T. Lee, H.H. Chen, C.H. Liao, C.H. Tsai, C.H. Chen, Appl. Phys. Lett. 85 (2004) 3301.
[21] H.L. Huang, K.H. Shen, M.C. Jhu, M.R. Tseng, J.M. Liu, Novel and efficient… materials MRS Proceedings 846 (2004) p.DD9.5, http://dx.doi.org/10.1557/PROC-846-DD9.5 2004.
[22] L. Xiao, Z. Chen, B. Qu, J. Luo, S. Kong, Q. Gong, J. Kido, Adv. Mater. 23 (2011) 926.
[23] Q. Wang, J. Ding, D. Ma, Y. Cheng, L. Wang, X. Jing, F. Wang, Adv. Func.l Mater. 19 (2009) 84.
[24] R.J. Holmes, S.R. Forrest, Y.J. Tung, R.C. Kwong, J.J. Brown, S. Garon M.E. Thompson, Appl. Phys. Lett. 82 (2003) 2422.
[25] G. Schwartz, K. Fehse, M. Pfeiffer, K. Walzer, K. Leo, Appl. Phys. Lett. 89 (2006) 083509.
[26] M.A. Baldo, M.E. Thompson, S.R. Forrest, Nature 403 (2000) 750.
[27] C. Han, G. Xie, H. Xu, Z. Zhang, D. Yu, Y. Zhao, P. Yan, Z. Deng, Q. Li, S. Liu, Chem. — Eur. J. 17 (2011) 445.
[28] J. Huang, M. Pfeiffer, A. Werner, J. Blochwitz, K. Leo, S. Liu, Appl. Phys. Lett. 80 (2002) 139.